

Scalable Gaussian Process Classification with Additive Noise for Various Likelihoods

Haitao Liu, Yew-Soon Ong, *Fellow, IEEE*, Ziwei Yu, Jianfei Cai, *Senior Member, IEEE*, and Xiaobo Shen

Abstract—Gaussian process classification (GPC) provides a flexible and powerful statistical framework describing joint distributions over function space. Conventional GPCs however suffer from (i) poor scalability for big data due to the full kernel matrix, and (ii) intractable inference due to the non-Gaussian likelihoods. Hence, various scalable GPCs have been proposed through (i) the sparse approximation built upon a small inducing set to reduce the time complexity; and (ii) the approximate inference to derive analytical evidence lower bound (ELBO). However, these scalable GPCs equipped with analytical ELBO are limited to specific likelihoods or additional assumptions. In this work, we present a *unifying* framework which accommodates scalable GPCs using various likelihoods. Analogous to GP regression (GPR), we introduce additive noises to augment the probability space for (i) the GPCs with *step*, (multinomial) *probit* and *logit* likelihoods via the internal variables; and *particularly*, (ii) the GPC using *softmax* likelihood via the noise variables themselves. This leads to unified scalable GPCs with analytical ELBO by using variational inference. Empirically, our GPCs showcase better results than state-of-the-art scalable GPCs for extensive binary/multi-class classification tasks with up to two million data points.

Index Terms—Gaussian process classification, large-scale, additive noise, non-Gaussian likelihood, variational inference

I. INTRODUCTION

AS a non-parametric Bayesian model which is explainable and provides confidence in predictions, Gaussian process (GP) has been widely investigated and used in various scenarios, e.g., regression and classification [1], active learning [2], unsupervised learning [3], and multi-task learning [4], [5]. The central task in GP is to infer the latent function f , which follows a Gaussian process $\mathcal{GP}(0, k(\cdot))$ where the kernel $k(\cdot)$ describes the covariance among inputs, from n observations $\mathbf{X} = (\mathbf{x}_1, \dots, \mathbf{x}_n)^\top$ with labels $\mathbf{y} = (y_1, \dots, y_n)^\top$. The inference can be performed through the type-II maximum likelihood which maximizes over the model evidence $p(\mathbf{y})$.

We herein focus on GP classification (GPC) [6], [7] with discrete class labels. It is more challenging than the GP regression (GPR). Specifically, current GPC paradigms are facing two main challenges. The first is the poor scalability to tackle massive datasets. The inversion and determinant of the kernel matrix $\mathbf{K}_{nn} = k(\mathbf{X}, \mathbf{X}) \in R^{n \times n}$ incur $\mathcal{O}(n^3)$

time complexity for inference. This cubic complexity severely limits the applicability of GP, especially in the era of big data. It becomes more serious for multi-class classification, since we need to infer C latent functions for C classes. The second is the intractable inference for the posterior $p(\mathbf{f}|\mathbf{y})$ where \mathbf{f} is the latent function values at data points. Due to the commonly used non-Gaussian likelihoods $p(\mathbf{y}|\mathbf{f})$, e.g., the *step* likelihood, the (multinomial) *probit/logit* likelihoods and the *softmax* likelihood, the Bayesian rule $p(\mathbf{f}|\mathbf{y}) \propto p(\mathbf{y}|\mathbf{f})p(\mathbf{f})$ incurs however intractable inference.

Inspired by the success of scalable GPR in recent years [8]–[10], alternatively, we could address the two major issues in GPC by regarding the classification with discrete labels as a regression task. For example, we could either directly treat GPC as GPR, like [11]; or we interpret the class labels as the outputs of a Dirichlet distribution to encourage the GPR-like inference [12].

A more principled alternative is adopting the GPC framework to handle binary/multi-class cases. To address the inference issue, various approximate inference algorithms, e.g., laplace approximation (LA), expectation propagation (EP) and variational inference (VI), have been developed, the core of which is approximating the non-Gaussian $p(\mathbf{f}|\mathbf{y})$ with a tractable Gaussian $q(\mathbf{f})$ [13].

As for the scalability issue, it has been extensively exploited in the regime of GPR [14]. Particularly, the sparse approximations [9], [10], [15], [16] seek to distill the entire training data through a global inducing set $\{\mathbf{X}_m, \mathbf{u}\}$ comprising m ($m \ll n$) points, thus reducing the time complexity from $\mathcal{O}(n^3)$ to $\mathcal{O}(nm^2)$. This is achieved either by modifying the joint prior as $p(\mathbf{f}, f_*) \approx q(\mathbf{f}, f_*)$ where f_* is the latent function value at the test point \mathbf{x}_* [8]; or through directly approximating the posterior $p(\mathbf{f}|\mathbf{y}) \approx q(\mathbf{f})$ [9]. The time complexity can be further reduced to $\mathcal{O}(m^3)$ by recognizing an evidence lower bound (ELBO) for $\log p(\mathbf{y})$. The ELBO factorizes over data points [10], [17], [18], thus allowing efficient stochastic variational inference [19]. Moreover, by exploiting the specific structures, e.g., the Kronecker and Toeplitz structures, in the inducing set, the time complexity can be dramatically reduced to $\mathcal{O}(n)$ [16], [20], [21].

Hence, scalable GPCs could inherit the sparse framework from GPR, with the difficulty being that the model evidence or ELBO should be carefully built up in order to overcome the intractable Gaussian integrals. To this end, the fully independent training conditional (FITC) assumption $p(\mathbf{f}|\mathbf{u}) = \prod_{i=1}^n p(f_i|\mathbf{u})$ [15] is employed to build scalable

Haitao Liu is with the Rolls-Royce@NTU Corporate Lab, Nanyang Technological University, Singapore, 637460. E-mail: htliu@ntu.edu.sg.

Yew-Soon Ong and Jianfei Cai are with School of Computer Science and Engineering, Nanyang Technological University, Singapore, 639798. E-mail: oyewsoon@gmail.com, asjfc@ntu.edu.sg.

Ziwei Yu is with School of Computing, National University of Singapore, Singapore, 117417. Email: yuziwei@u.nus.edu.

Xiaobo Shen is with School of Computer Science and Engineering, Nanjing University of Science and Technology, China. Email: xbshen@njjust.edu.cn.

binary GPC [22].¹ The scalability has been further improved for binary/multi-class classification through the stochastic variants [24], [25], which derive a closed-form ELBO factorized over data points, thus supporting stochastic EP [26]. Differently, for binary classification, variational inference is adopted to derive a simple ELBO expressed as a one-dimensional Gaussian integral which can be calculated through Gauss-Hermite quadrature [27].² This model has been further extended to multi-class classification [28]. Particularly, when using the logit likelihood, the Pölya-Gamma data augmentation [29] can be used such that the ELBO and the posterior are analytical in the augmented probability space [30]. This augmentation strategy has been recently extended to multi-class classification using logistic-softmax likelihood [31].³ Besides, a decoupled approach [32], [33] from the weight-space view removes the coupling between the mean and the covariance of a GP, resulting in lower complexity and an expressive prediction mean.

Though showing high scalability for handling big data, existing scalable GPCs derive analytical ELBO (i) using additional assumptions which may limit the representational capability [24], [25], and (ii) only for specific likelihoods, e.g., the step or probit likelihood [25], [27], [30], [31], [33].

Hence, this article proposes a unifying scalable GPC framework which accommodates various likelihoods without additional assumptions. Specifically, by interpreting the GPC as a noisy model analogous to GPR, we describe the step and (multinomial) probit/logit likelihoods over a general Gaussian error, and the softmax likelihood over a Gumbel error. Thereafter, we augment the probability space for (i) the GPCs using *step* and (multinomial) *probit/logit* likelihoods via the internal variables; and *particularly*, (ii) the GPC using *softmax* likelihood via the noises themselves. This leads to scalable GPCs with analytical ELBO by using variational inference. We empirically demonstrate the superiority of our GPCs on extensive binary/multi-class classification tasks with up to two million data points. Python implementations built upon the GPflow library [34] are available at <https://github.com/LiuHaiTao01/GPCnoise>.

The reminder of this article is organized as follows. We introduce the proposed scalable binary/multi-class GPCs with additive noise in sections II and III, respectively. Thereafter, section IV conducts numerical experiments to assess the performance of proposed GPCs against state-of-the-art GPCs. Finally, section V offers concluding remarks.

II. BINARY GPCs WITH ADDITIVE NOISE

A. Interpreting binary GPCs with additive noise

For the binary classification with $y \in \{-1, 1\}$, the GPC model in Fig. 1(a) is usually expressed as

$$f(\mathbf{x}) \sim \mathcal{GP}(0, k(\mathbf{x}, \mathbf{x}')), \quad p(y|f) = \pi(yf), \quad (1)$$

¹For GPR, this assumption severely underestimates the noise variance and worsens the prediction mean [23].

²Due to the fast Gauss-Hermite quadrature with high precision, this ELBO is regarded as analytical.

³Different from the original softmax likelihood, this hybrid likelihood allows deriving analytical ELBO via a complex three-level augmentation.

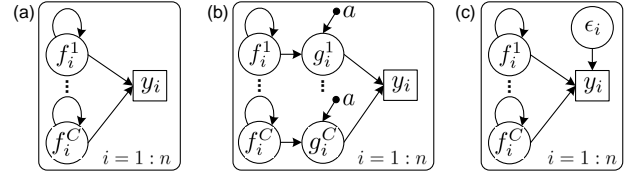


Fig. 1. (a) Illustration of the GPC where for binary case $C = 1$ and for multi-class case $C > 2$. (b) The GPC with additive Gaussian noise $\epsilon_i^c \in \mathcal{N}(0, a)$. This model is augmented by introducing the internal function g , which offers a unifying description and helps derive closed-form ELBO. By marginalizing g out and varying over a , we recover the GPC in (a) using step and (multinomial) probit/logit likelihoods. (c) Particularly, for multi-class GPC using softmax likelihood, instead of introducing g , we directly use the Gumbel error ϵ_i to augment the probability space for deriving analytical ELBO.

where the likelihood $p(y|f)$ employs an inverse link function $\pi(\cdot) \in [0, 1]$ to squash the latent function f into the class probability space. Commonly used $\pi(\cdot)$ for binary GPC includes

$$\begin{aligned} \text{step} : \pi(z) &= H(z), \\ \text{probit} : \pi(z) &= \int_{-\infty}^z \mathcal{N}(\tau|0, 1) d\tau, \\ \text{logit} : \pi(z) &= (1 + \exp(-z))^{-1}, \end{aligned} \quad (2)$$

where $H(z) = 1$ when $z > 0$; otherwise, $H(z) = 0$.

It is known that similar to the GPR $y(\mathbf{x}) = f(\mathbf{x}) + \epsilon(\mathbf{x})$, the GPC in (1) can also be interpreted as a noisy model. Specifically, we introduce a GPR-like internal latent function g and the internal step likelihood, resulting in

$$g(\mathbf{x}) = f(\mathbf{x}) + \epsilon(\mathbf{x}), \quad p(y|g) = H(yg), \quad (3)$$

where $\epsilon(\mathbf{x})$ is an independent and identically distributed (*i.i.d.*) noise which follows a distribution with probability density function (PDF) $\phi(\cdot)$ and cumulative distribution function (CDF) $\Phi(\cdot)$. The additional variable g in (3) augments the probability space, and incurs the conditional independence $y \perp f|g$, which is crucial for deriving the analytical ELBO below.

The conventional likelihoods in (2) can be recovered by marginalizing the internal g out as⁴

$$p(y|f) = \int p(y|g)p(g|f)dg = \Phi(yf). \quad (4)$$

It is observed that (i) when ϵ follows the Dirac-delta distribution $\phi_{\mathcal{D}}(\epsilon)$ which is zero everywhere except at the origin where it is infinite, Eq. (4) recovers the step likelihood; (ii) when ϵ follows the normal distribution $\phi_{\mathcal{N}}(\epsilon|0, 1)$, Eq. (4) recovers the probit likelihood; and finally, (iii) when ϵ follows the standard logistic distribution $\phi_{\mathcal{L}}(\epsilon|0, 1)$, Eq. (4) recovers the logit likelihood.

More interestingly, we could use a general Gaussian error $\epsilon \sim \mathcal{N}(0, a)$ to describe the above three kinds of errors in a unifying way, since all of them are *symmetric, bell-shaped* distributions. It is observed that (i) when $a \rightarrow 0$, the Gaussian error degenerates to the Dirac-delta error;⁵ (ii) when $a = 1$,

⁴Eq. (4) holds only when ϵ follows a symmetric distribution, i.e., $\Phi(x) = 1 - \Phi(-x)$. Otherwise, we have $p(y = 1|f) = 1 - \Phi(-f)$ and $p(y = -1|f) = \Phi(-f)$.

⁵Directly using $a = 0$ will incur numerical issue for $\phi_{\mathcal{N}}(\cdot)$ and $\Phi_{\mathcal{N}}(\cdot)$. But this issue can be sidestepped in the GPC model presented below.

the Gaussian error is equivalent to the normal error; and (iii) when $a = 2.897$, the Gaussian error produces a well CDF approximation to that of the logistic error with the maximum difference as 0.009, see Fig. 5 in Appendix A. Bowling and Khasawneh [35] proposed using the logistic function to approximate the normal CDF $\Phi_{\mathcal{N}}$. Inversely, we here use the Gaussian error to approximate the logistic error. Note that the optimal a for logistic error is derived in terms of CDF rather than PDF since we focus on the approximation quality of the likelihood (4).

Now the internal model $g(\mathbf{x}) = f(\mathbf{x}) + \mathcal{N}(\epsilon|0, a)$ with additive Gaussian noise, as depicted in Fig. 1(b), helps (i) describe the binary GPCs using different likelihoods uniformly; and moreover, (ii) derive unifying and analytical ELBO and prediction in section II-B.

B. Binary GPCs using step, probit and logit likelihoods

1) *Evidence lower bound*: Different from (3), we here introduce a robust parameter δ like [36], resulting in the likelihoods

$$\begin{aligned} p(y|g) &= (1 - 2\delta)H(yg) + \delta, \\ p(y|f) &= (1 - 2\delta)\Phi_{\mathcal{N}}\left(\frac{yf}{\sqrt{a}}\right) + \delta. \end{aligned} \quad (5)$$

The parameter δ , which is pretty small (e.g., 10^{-3}), (i) prevents the ELBO below from being infinite, which is caused by the logarithm form $\log p(y|g)$; and (ii) gives a degree of robustness to outliers. Note that with δ , $p(y|g)$ is still a distribution since we have $p(y|g) = \{1 - \delta, \delta\}$.

Given the data $\{\mathbf{X}, \mathbf{y}\}$ we have the joint prior $p(\mathbf{f}) = \mathcal{N}(\mathbf{f}|\mathbf{0}, \mathbf{K}_{nn})$ where $\mathbf{f} = (f_1, \dots, f_n)^\top$ and $[\mathbf{K}_{nn}]_{ij} = k(\mathbf{x}_i, \mathbf{x}_j)$. Thereafter, we have the likelihoods $p(\mathbf{g}|\mathbf{f}) = \mathcal{N}(\mathbf{g}|\mathbf{f}, a\mathbf{I})$ and $p(\mathbf{y}|\mathbf{g}) = \prod_{i=1}^n p(y_i|g_i)$. To improve the scalability for dealing with big data, we consider m inducing variables \mathbf{u} , which follow the same GP prior $p(\mathbf{u}) = \mathcal{N}(\mathbf{u}|\mathbf{0}, \mathbf{K}_{mm})$, for the latent variables \mathbf{f} .⁶ In the statistical model, a central task is deriving the posterior $p(\mathbf{g}, \mathbf{f}, \mathbf{u}|\mathbf{y}) \propto p(\mathbf{y}|\mathbf{g})p(\mathbf{g}|\mathbf{f})p(\mathbf{f}|\mathbf{u})$ given the observations. It however is intractable for GPC due to the non-Gaussian likelihood $p(\mathbf{y}|\mathbf{g})$.

Instead, we introduce a variational distribution $q(\mathbf{g}, \mathbf{f}, \mathbf{u}) = p(\mathbf{g}|\mathbf{f})p(\mathbf{f}|\mathbf{u})q(\mathbf{u})$ ⁷ to approximate the exact posterior $p(\mathbf{g}, \mathbf{f}, \mathbf{u}|\mathbf{y})$. We then minimize their KL divergence $\text{KL}(q(\mathbf{g}, \mathbf{f}, \mathbf{u})||p(\mathbf{g}, \mathbf{f}, \mathbf{u}|\mathbf{y})) = \log p(\mathbf{y}) - \mathcal{L}$, which is equivalent to maximizing the evidence lower bound (ELBO) \mathcal{L} expressed as

$$\begin{aligned} \mathcal{L} &= \left\langle \log \frac{p(\mathbf{y}, \mathbf{g}, \mathbf{f}, \mathbf{u})}{q(\mathbf{g}, \mathbf{f}, \mathbf{u})} \right\rangle_{q(\mathbf{g}, \mathbf{f}, \mathbf{u})} \\ &= \langle \log p(\mathbf{y}|\mathbf{g}) \rangle_{q(\mathbf{g})} - \text{KL}(q(\mathbf{u})||p(\mathbf{u})), \end{aligned} \quad (6)$$

where $\langle \cdot \rangle_{q(\cdot)}$ is the expectation over distribution $q(\cdot)$, and $q(\mathbf{g}) = \int p(\mathbf{g}|\mathbf{f})p(\mathbf{f}|\mathbf{u})q(\mathbf{u})d\mathbf{f}d\mathbf{u} = \int p(\mathbf{g}|\mathbf{f})q(\mathbf{f})d\mathbf{f}$. For the GPR-like internal model $g(\mathbf{x}) = f(\mathbf{x}) + \mathcal{N}(\epsilon|0, a)$, we could

⁶ \mathbf{u} is assumed to be a sufficient statistic for \mathbf{f} , i.e., for any \mathbf{z} we have $p(\mathbf{z}|\mathbf{u}, \mathbf{f}) = p(\mathbf{z}|\mathbf{u})$.

⁷According to [9], we have $p(\mathbf{z}|\mathbf{u}, \mathbf{y}) = p(\mathbf{z}|\mathbf{u})$. Hence, $q(\mathbf{g}, \mathbf{f}, \mathbf{u}) = p(\mathbf{g}, \mathbf{f}|\mathbf{u}, \mathbf{y})q(\mathbf{u}) = p(\mathbf{g}, \mathbf{f}|\mathbf{u})q(\mathbf{u}) = p(\mathbf{g}|\mathbf{f})p(\mathbf{f}|\mathbf{u})q(\mathbf{u})$.

derive an analytical posterior $q(\mathbf{g})$. Specifically, given that $q(\mathbf{u}) = \mathcal{N}(\mathbf{u}|\mathbf{m}, \mathbf{S})$, we have

$$\begin{aligned} q(\mathbf{f}) &= \int p(\mathbf{f}|\mathbf{u})q(\mathbf{u})d\mathbf{u} = \mathcal{N}(\mathbf{f}|\boldsymbol{\mu}_f, \boldsymbol{\Sigma}_f), \\ q(\mathbf{g}) &= \int p(\mathbf{g}|\mathbf{f})q(\mathbf{f})d\mathbf{f} = \mathcal{N}(\mathbf{g}|\boldsymbol{\mu}_g, \boldsymbol{\Sigma}_g), \end{aligned} \quad (7)$$

where $\boldsymbol{\mu}_f = \mathbf{K}_{nm}\mathbf{K}_{mm}^{-1}\mathbf{m}$, $\boldsymbol{\Sigma}_f = \mathbf{K}_{nn} + \mathbf{K}_{nm}\mathbf{K}_{mm}^{-1}[\mathbf{S}\mathbf{K}_{mm}^{-1} - \mathbf{I}]\mathbf{K}_{mn}$, $\boldsymbol{\mu}_g = \boldsymbol{\mu}_f$ and $\boldsymbol{\Sigma}_g = a\mathbf{I} + \boldsymbol{\Sigma}_f$. Inserting (7) back into (6), we obtain a closed-form ELBO factorized over data points as

$$\begin{aligned} \mathcal{L} &= \sum_{i=1}^n \left[\log \left(\frac{1 - \delta}{\delta} \right) \Phi_{\mathcal{N}} \left(\frac{y_i \mu_{f_i}}{\sqrt{a + \nu_{f_i}}} \right) + \log \delta \right] \\ &\quad - \text{KL}(q(\mathbf{u})||p(\mathbf{u})), \end{aligned} \quad (8)$$

where $\mu_{f_i} = [\boldsymbol{\mu}_f]_i$ and $\nu_{f_i} = [\boldsymbol{\Sigma}_f]_{ii}$. The maximization of \mathcal{L} permits inferring the variational parameters and hyperparameters simultaneously. Besides, the sum term in the right-hand side of \mathcal{L} allows using efficient stochastic optimizer, e.g., the Adam [37], for model training.⁸

It is observed from (8) that (i) when $a = 0$, we obtain the bound \mathcal{L} for the binary GPC using step likelihood; (i) when $a = 1$, we obtain the binary GPC using probit likelihood; and (i) when $a = 2.897$, we obtain the binary GPC using logit likelihood. The unifying bound (8) reveals that the binary GPCs using step, probit and logit likelihoods have similar behavior.

2) *Prediction*: The prediction for f_* at \mathbf{x}_* is $p(f_*|\mathbf{y}) = \int p(f_*|\mathbf{f})q(\mathbf{f})d\mathbf{f} = \mathcal{N}(f_*|\mu_{f_*}, \nu_{f_*})$, where $\mu_{f_*} = \mathbf{k}_{*m}\mathbf{K}_{mm}^{-1}\mathbf{m}$, and $\nu_{f_*} = k_{**} + \mathbf{k}_{*m}\mathbf{K}_{mm}^{-1}[\mathbf{S}\mathbf{K}_{mm}^{-1} - \mathbf{I}]\mathbf{k}_{m*}$. Similarly, we obtain the prediction for g_* at \mathbf{x}_* as $p(g_*|\mathbf{y}) = \int p(g_*|\mathbf{g})q(\mathbf{g})d\mathbf{g} = \mathcal{N}(g_*|\mu_{g_*}, \nu_{g_*})$, where $\mu_{g_*} = \mu_{f_*}$ and $\nu_{g_*} = \nu_{f_*} + a$. Finally, we have the closed-form class probability for $y_* = 1$ as

$$\begin{aligned} p(y_* = 1|\mathbf{y}) &= \int p(y_* = 1|g_*)p(g_*|\mathbf{y})df_* \\ &= (1 - 2\delta)\Phi_{\mathcal{N}}\left(\frac{\mu_{f_*}}{\sqrt{a + \nu_{f_*}}}\right) + \delta. \end{aligned} \quad (9)$$

C. Discussions

We would like to emphasize that the binary GPCs proposed in section II-B are different from that in section 3.2 of [27]. Hensman et al. [27] borrowed the bound \mathcal{L}_g for $\log p(\mathbf{g})$ in [10], which is equivalent to maximizing $\text{KL}(q(\mathbf{f}, \mathbf{u}|\mathbf{g})||p(\mathbf{f}, \mathbf{u}|\mathbf{g}))$, and substituted it into the augmented joint distribution $p(\mathbf{y}, \mathbf{g}, \mathbf{f})$. This results in $\log p(\mathbf{y}) \geq \log \int p(\mathbf{y}|\mathbf{g}) \exp(\mathcal{L}_g)d\mathbf{g} = \mathcal{L}_{\text{HS}}$. When using robust $p(\mathbf{y}|\mathbf{g})$, we have

$$\begin{aligned} \mathcal{L}_{\text{HS}} &= \sum_{i=1}^n \log((1 - 2\delta)\Phi_{\mathcal{N}}(y_i \mu_{f_i}) + \delta) - \frac{1}{2}\text{tr}(\boldsymbol{\Sigma}_f) \\ &\quad - \text{KL}(q(\mathbf{u})||p(\mathbf{u})), \end{aligned} \quad (10)$$

⁸Particularly, the natural gradient descent (NGD) could be employed for optimizing the variational parameters \mathbf{m} and \mathbf{S} . But in comparison to GPR, the NGD+Adam optimizer brings little benefits for classification [33], [38].

which is different from our bound (8). Let $\mathbf{X}_m = \mathbf{X}$ so that $\mathbf{u} = \mathbf{f}$, \mathcal{L}_{HS} has a unique optimum where $\mathbf{m}_* = \mathbf{K}_{nn} \partial \alpha(\mathbf{m}) / \partial \mathbf{m}$ and $\mathbf{S}_* = (\mathbf{K}_{nn}^{-1} + \mathbf{I})^{-1}$ with $\alpha(\mathbf{m})$ being the first term in the right-hand side of \mathcal{L}_{HS} . The ineffective estimations \mathbf{m}_* and \mathbf{S}_* are not due to the decoupling $y \perp f | g$. They occur since \mathcal{L}_{HS} seeks to infer $q(\mathbf{f} | \mathbf{g})$ rather than the interested $q(\mathbf{f} | \mathbf{y})$.

In contrast, our binary GPCs use VI to directly approximate $\log p(\mathbf{y})$ via maximizing $\text{KL}(q(\mathbf{g}, \mathbf{f}, \mathbf{u} | \mathbf{y}) || p(\mathbf{g}, \mathbf{f}, \mathbf{u} | \mathbf{y}))$. The improvement occurs that the internal variables \mathbf{g} and the general Gaussian error help derive completely analytical ELBOs for binary GPCs using step, probit and logit likelihoods. Let $\mathbf{X}_m = \mathbf{X}$, our bound \mathcal{L} in (8) has a unique optimum where $\mathbf{m}_* = \mathbf{K}_{nn} \partial \beta(a, \mathbf{m}, \mathbf{S}) / \partial \mathbf{m}$ and $\mathbf{S}_* = (\mathbf{K}_{nn}^{-1} - 2 \times \partial \beta(a, \mathbf{m}, \mathbf{S}) / \partial \mathbf{S})^{-1}$ with β being the first term in the right-hand side of \mathcal{L} . This optimum, which is similar to that of the KL method rather than the Laplace approximation in [13], is more informative than that of \mathcal{L}_{HS} .

III. MULTI-CLASS GPCs WITH ADDITIVE NOISE

A. Interpreting multi-class GPCs with additive noise

The more complicated multi-class GPC with the label $y \in \{1, \dots, C\}$, $C > 2$, is expressed by introducing the internals $\{g^c\}_{c=1}^C$ for each of the C classes as

$$\begin{aligned} f^c(\mathbf{x}) &\sim \mathcal{GP}(0, k^c(\mathbf{x}, \mathbf{x}')), \\ g^c(\mathbf{x}) &= f^c(\mathbf{x}) + \epsilon^c(\mathbf{x}), \\ y(\mathbf{x}) &= \underset{c}{\text{argmax}} g^c(\mathbf{x}), \end{aligned} \quad (11)$$

where f^c and g^c are independent latent functions, and ϵ^c is the *i.i.d.* noise for class c ($1 \leq c \leq C$). For notations, we first define $\mathbf{f}_i = (f^1(\mathbf{x}_i), \dots, f^C(\mathbf{x}_i))^T \in R^C$, $\mathbf{f}^c = (f^c(\mathbf{x}_1), \dots, f^c(\mathbf{x}_n))^T \in R^n$, $\mathbf{f} = (\mathbf{f}^1, \dots, \mathbf{f}^C) \in R^{n \times C}$, $\mathbf{g}_i = (g^1(\mathbf{x}_i), \dots, g^C(\mathbf{x}_i))^T \in R^C$, $\mathbf{g}^c = (g^c(\mathbf{x}_1), \dots, g^c(\mathbf{x}_n))^T \in R^n$, and $\mathbf{g} = (\mathbf{g}^1, \dots, \mathbf{g}^C) \in R^{n \times C}$. We adopt the internal step likelihood

$$p(y_i | \mathbf{g}_i) = \prod_{c \neq y_i} H(g_i^{y_i} - g_i^c) = \prod_{c \neq y_i} H(f_i^{y_i} + \epsilon_i^{y_i} - f_i^c - \epsilon_i^c). \quad (12)$$

Thereafter, by integrating \mathbf{g}_i out, we obtain the conventional likelihood⁹

$$\begin{aligned} p(y_i | \mathbf{f}_i) &= \int p(y_i | \mathbf{g}_i) p(\mathbf{g}_i | \mathbf{f}_i) d\mathbf{g}_i \\ &= \int \phi(\epsilon_i) \prod_{c \neq y_i} \Phi(\epsilon_i + f_i^{y_i} - f_i^c) d\epsilon_i. \end{aligned} \quad (13)$$

It is observed that (i) when $\epsilon_i \sim \phi_{\mathcal{D}}(\epsilon)$, Eq. (13) recovers the multi-class step likelihood; (ii) when $\epsilon_i \sim \phi_{\mathcal{N}}(\epsilon | 0, 1)$, Eq. (13) recovers the multinomial probit likelihood; (iii) when $\epsilon_i \sim \phi_{\mathcal{L}}(\epsilon | 0, 1)$, Eq. (13) recovers the multinomial logit likelihood; and finally, (iv) when using the Gumbel error $\epsilon_i \sim \phi_{\mathcal{G}}(\epsilon | 0, 1)$, Eq. (13) recovers the softmax likelihood, i.e.,

$$p(y_i | \mathbf{f}_i) = \frac{\exp(f_i^{y_i})}{\sum_{c=1}^C \exp(f_i^c)}. \quad (14)$$

⁹We omit the superscript in $\epsilon_i^{y_i}$ since Eq. (13) has removed the dependency on other error terms $\{\epsilon_i^c\}_{c \neq y_i}$.

Similarly, as depicted in Fig. 1(b), we can employ a Gaussian error $\epsilon \sim \mathcal{N}(0, a)$ to describe the first three symmetric errors with $a \rightarrow 0$, $a = 1$, and $a = 2.897$, respectively. But this is not the case for the *asymmetric* Gumbel error, see Fig. 5 in Appendix A. Hence, section III-B introduces the sparse multi-class GPCs using step and multinomial probit/logit likelihoods in a unifying framework; *particularly*, section III-D introduces the sparse multi-class GPC using softmax likelihood.

B. Multi-class GPCs using step and multinomial probit/logit likelihoods

1) *Evidence lower bound*: Similar to (5), we employ the robust likelihoods as

$$\begin{aligned} p(y_i | \mathbf{g}_i) &= \left(1 - \frac{C}{C-1} \delta\right) \prod_{c \neq y_i} H(g_i^{y_i} - g_i^c) + \frac{\delta}{C-1}, \\ p(y_i | \mathbf{f}_i) &= (1 - \frac{C}{C-1} \delta) S_0 + \frac{\delta}{C-1}, \end{aligned} \quad (15)$$

where, given that $p(\mathbf{g}_i | \mathbf{f}_i) = \mathcal{N}(\mathbf{g}_i | \mathbf{f}_i, a\mathbf{I})$, $S_0 = \mathbb{E}_{\epsilon_i \sim \mathcal{N}(0, a)} \left[\prod_{c \neq y_i} \Phi_{\mathcal{N}} \left(\frac{\epsilon_i + f_i^{y_i} - f_i^c}{\sqrt{a}} \right) \right]$.

Again, by introducing the independent inducing set \mathbf{u}^c for \mathbf{f}^c , $1 \leq c \leq C$, the ELBO writes

$$\begin{aligned} \mathcal{L} &= \left\langle \log \frac{p(\mathbf{y}, \mathbf{g}, \mathbf{f}, \mathbf{u})}{q(\mathbf{g}, \mathbf{f}, \mathbf{u})} \right\rangle_{q(\mathbf{g}, \mathbf{f}, \mathbf{u})} \\ &= \langle \log p(\mathbf{y} | \mathbf{g}) \rangle_{q(\mathbf{g})} - \sum_{c=1}^C \text{KL}(q(\mathbf{u}^c) || p(\mathbf{u}^c)). \end{aligned} \quad (16)$$

Let $q(\mathbf{u}^c) = \mathcal{N}(\mathbf{u}^c | \mathbf{m}^c, \mathbf{S}^c)$, we have

$$\begin{aligned} q(\mathbf{f}) &= \int p(\mathbf{f} | \mathbf{u}) q(\mathbf{u}) d\mathbf{u} = \prod_{c=1}^C \mathcal{N}(\mathbf{f}^c | \boldsymbol{\mu}_f^c, \boldsymbol{\Sigma}_f^c), \\ q(\mathbf{g}) &= \int p(\mathbf{g} | \mathbf{f}) q(\mathbf{f}) d\mathbf{f} = \prod_{c=1}^C \mathcal{N}(\mathbf{g}^c | \boldsymbol{\mu}_g^c, \boldsymbol{\Sigma}_g^c), \end{aligned} \quad (17)$$

where $\boldsymbol{\mu}_f^c = \mathbf{K}_{nm}^c (\mathbf{K}_{mm}^c)^{-1} \mathbf{m}^c$, $\boldsymbol{\Sigma}_f^c = \mathbf{K}_{nn}^c + \mathbf{K}_{nm}^c (\mathbf{K}_{mm}^c)^{-1} [\mathbf{S}^c (\mathbf{K}_{mm}^c)^{-1} - \mathbf{I}] \mathbf{K}_{mn}^c$, $\boldsymbol{\mu}_g^c = \boldsymbol{\mu}_f^c$ and $\boldsymbol{\Sigma}_g^c = a\mathbf{I} + \boldsymbol{\Sigma}_f^c$. Inserting (17) back into (16), we have a factorized ELBO as

$$\begin{aligned} \mathcal{L} &= \sum_{i=1}^n \left[\log(1 - \delta) S_i + \log \left(\frac{\delta}{C-1} \right) (1 - S_i) \right] \\ &\quad - \sum_{c=1}^C \text{KL}(q(\mathbf{u}^c) || p(\mathbf{u}^c)). \end{aligned} \quad (18)$$

where $S_i = \mathbb{E}_{g_i^{y_i} \sim \mathcal{N}(\mu_{f_i}^{y_i}, a + \nu_{f_i}^{y_i})} \left[\prod_{c \neq y_i} \Phi_{\mathcal{N}} \left(\frac{g_i^{y_i} - \mu_{f_i}^c}{\sqrt{a + \nu_{f_i}^c}} \right) \right]$. The term S_i is interpreted as the probability that the function value corresponding to the observed class y_i is larger than the others at \mathbf{x}_i . Note that this *one dimensional Gaussian integral* can be evaluated using fast Gauss-Hermite quadrature with high precision.

The unifying ELBO (18) herein describes the multi-class GPCs using step likelihood ($a = 0$), multinomial probit likelihood ($a = 1$) and multinomial logit likelihood ($a = 2.897$). Note that when $a = 0$, the model is equivalent to the one presented in [36].

2) *Prediction*: Finally, the prediction for $\mathbf{f}_* = (f_*^1, \dots, f_*^C)^\top$ at \mathbf{x}_* is $p(\mathbf{f}_*|\mathbf{y}) = \int p(\mathbf{f}_*|\mathbf{f})q(\mathbf{f})d\mathbf{f} = \prod_{c=1}^C \mathcal{N}(f_*^c|\mu_{f_*}^c, \nu_{f_*}^c)$, where $\mu_{f_*}^c = \mathbf{k}_{*m}^c(\mathbf{K}_{mm}^c)^{-1}\mathbf{m}^c$ and $\nu_{f_*}^c = k_{**}^c + \mathbf{k}_{*m}^c(\mathbf{K}_{mm}^c)^{-1}[\mathbf{S}^c(\mathbf{K}_{mm}^c)^{-1} - \mathbf{I}]\mathbf{k}_{m*}^c$. Similarly, we have the prediction for \mathbf{g}_* at \mathbf{x}_* as $p(\mathbf{g}_*|\mathbf{y}) = \int p(\mathbf{g}_*|\mathbf{g})q(\mathbf{g})d\mathbf{g} = \prod_{c=1}^C \mathcal{N}(g_*^c|\mu_{g_*}^c, \nu_{g_*}^c)$, where $\mu_{g_*}^c = \mu_{f_*}^c$ and $\nu_{g_*}^c = \nu_{f_*}^c + a$. Finally, we have

$$\begin{aligned} p(y_*|\mathbf{y}) &= \int p(y_*|\mathbf{g}_*)p(\mathbf{g}_*|\mathbf{y})d\mathbf{f}_* \\ &= (1 - \delta)S_* + \frac{\delta}{C-1}(1 - S_*), \end{aligned} \quad (19)$$

$$\text{where } S_* = \mathbb{E}_{g_*^{y_*} \sim \mathcal{N}(\mu_{f_*}^{y_*}, a + \nu_{f_*}^{y_*})} \left[\prod_{c \neq y_*} \Phi_{\mathcal{N}} \left(\frac{g_*^{y_*} - \mu_{f_*}^c}{\sqrt{a + \nu_{f_*}^c}} \right) \right].$$

C. A possible generalization?

It is found that the *unifying* ELBOs in (8) and (18) respectively recover the binary and multi-class GPCs using step and (multinomial) probit/logit likelihoods by varying over the Gaussian noise variance a . It indicates that the GPCs using these three *symmetric* likelihoods would produce similar results, which will be verified in the numerical experiments in section IV.

Besides, the parameter a inspires us to think of a more general GPC model, like standard GPR, by treating the variance a as a hyperparameter and inferring it from data. However, as discussed in Appendix B, the ELBOs in (8) and (18) increase with decreasing a . That means, \mathcal{L} arrives at the maximum with $a = 0$. This is because the internal likelihood $p(\mathbf{y}|\mathbf{g})$ does not take into account the noise variance.

We name the GPCs using step and (multinomial) probit/logit likelihoods as GPC-I, GPC-II and GPC-III, respectively. It is found that given the same configuration of hyperparameters, the ELBO satisfies $\mathcal{L}_I > \mathcal{L}_{II} > \mathcal{L}_{III}$, which again verifies that the noise variance a is not a proper hyperparameter.

D. Multi-class GPC using softmax likelihood

1) *Evidence lower bound*: According to (13), the softmax likelihood used in the noisy multi-class GPC is equivalent to

$$p(y_i|\mathbf{f}_i) = \int \phi_{\mathcal{G}}(\epsilon_i) \prod_{c \neq y_i} \Phi_{\mathcal{G}}(\epsilon_i + f_i^{y_i} - f_i^c) d\epsilon_i, \quad (20)$$

where for the standard Gumbel error, the PDF is $\phi_{\mathcal{G}}(x) = \exp(-x - e^{-x})$ and the CDF is $\Phi_{\mathcal{G}}(x) = \exp(-e^{-x})$. Instead of introducing the internal \mathbf{g} , we here directly use the noise variables $\epsilon = \{\epsilon_i\}_{i=1}^n$ to augment the probability space due to the expectation form in (20), as depicted in Fig. 1(c). Hence, the augmented model with ϵ_i has the following conditional distributions as

$$\begin{aligned} p(y_i, \epsilon_i|\mathbf{f}_i) &= \phi_{\mathcal{G}}(\epsilon_i) \prod_{c \neq y_i} \Phi_{\mathcal{G}}(\epsilon_i + f_i^{y_i} - f_i^c), \\ p(y_i|\epsilon_i, \mathbf{f}_i) &= \prod_{c \neq y_i} \Phi_{\mathcal{G}}(\epsilon_i + f_i^{y_i} - f_i^c). \end{aligned} \quad (21)$$

By introducing the inducing set \mathbf{u}^c for \mathbf{f}^c , $1 \leq c \leq C$, we derive the ELBO as

$$\begin{aligned} \mathcal{L} &= \left\langle \log \frac{p(\mathbf{y}, \mathbf{f}, \mathbf{u}, \epsilon)}{q(\mathbf{f}, \mathbf{u}, \epsilon)} \right\rangle_{q(\mathbf{f}, \mathbf{u}, \epsilon)} \\ &= \sum_i^n \langle \log p(y_i|\mathbf{f}_i, \epsilon_i) \rangle_{q(\mathbf{f}_i)q(\epsilon_i|\mathbf{f}_i)} - \sum_{i=1}^n \text{KL}(q(\epsilon_i|\mathbf{f}_i)||p(\epsilon_i)) \\ &\quad - \sum_{c=1}^C \text{KL}(q(\mathbf{u}^c|\mathbf{y})||p(\mathbf{u}^c)), \end{aligned} \quad (22)$$

where $q(\mathbf{f}, \mathbf{u}, \epsilon) = p(\mathbf{f}|\mathbf{u})q(\mathbf{u})q(\epsilon|\mathbf{f})$; $q(\mathbf{f}_i) = \prod_{c=1}^C q(f_i^c) = \prod_{c=1}^C \mathcal{N}(f_i^c|\mu_{f_i}^c, \nu_{f_i}^c)$ with $\mu_{f_i}^c = [\boldsymbol{\mu}_f^c]_i$ and $\nu_{f_i}^c = [\boldsymbol{\Sigma}_f^c]_{ii}$; and $q(\epsilon_i|\mathbf{f}_i)$ approximates the posterior $p(\epsilon_i|y_i, \mathbf{f}_i)$, which follows the exact expression as

$$\begin{aligned} p(\epsilon_i|y_i, \mathbf{f}_i) &\propto p(y_i|\mathbf{f}_i, \epsilon_i)p(\epsilon_i) \\ &= \phi_{\mathcal{G}}(\epsilon_i) \prod_{c \neq y_i} \Phi_{\mathcal{G}}(\epsilon_i + f_i^{y_i} - f_i^c) \\ &= \exp \left(-\epsilon_i - \left(1 + \sum_{c \neq y_i} e^{f_i^c - f_i^{y_i}} \right) e^{-\epsilon_i} \right) \\ &\stackrel{\text{c}}{=} \text{Gumbel}(\epsilon_i | \log \theta_i^*, 1), \end{aligned} \quad (23)$$

where $\theta_i^* = 1 + \sum_{c \neq y_i} e^{f_i^c - f_i^{y_i}} = \sum_{c=1}^C e^{f_i^c - f_i^{y_i}}$. Note that though the optimal $p(\epsilon_i|y_i, \mathbf{f}_i)$ has an analytic form, directly using $p(\epsilon_i|y_i, \mathbf{f}_i)$ will make the ELBO intractable. Hence, we adopt a general distribution $q(\epsilon_i|\mathbf{f}_i) = \text{Gumbel}(\epsilon_i | \log \theta_i, 1)$ which satisfies $\theta_i > 1$ and already contains the optimal distribution.

Thereafter, the closed-form ELBO, which is detailed in Appendix C, is reorganized as,

$$\mathcal{L} = \sum_{i=1}^n \left\{ -\frac{1}{\theta_i} \mathcal{P}_i - \log \theta_i - \frac{1}{\theta_i} + 1 \right\} - \sum_{c=1}^C \text{KL}(q(\mathbf{u}^c|\mathbf{y})||p(\mathbf{u}^c)), \quad (24)$$

where $\mathcal{P}_i = \exp \left(\frac{\nu_{f_i}^{y_i}}{2} - \mu_{f_i}^{y_i} \right) \sum_{c \neq y_i} \exp \left(\frac{\nu_{f_i}^c}{2} + \mu_{f_i}^c \right)$. Furthermore, in order to obtain a tight bound, let the derivative of \mathcal{L} w.r.t. θ_i

$$\frac{\partial \mathcal{L}}{\partial \theta_i} = \frac{1}{\theta_i^2} (\mathcal{P}_i + 1) - \frac{1}{\theta_i}$$

to be zero, we have the optimal value $\theta_i^* = \mathcal{P}_i + 1$. Substituting θ_i^* into \mathcal{L} , we have

$$\mathcal{L} = - \sum_{i=1}^n \log(\mathcal{P}_i + 1) - \sum_{c=1}^C \text{KL}(q(\mathbf{u}^c|\mathbf{y})||p(\mathbf{u}^c)). \quad (25)$$

We here name the GPC using softmax likelihood as GPCsm.

2) *Prediction*: To predict the latent function values \mathbf{f}_* at the test point \mathbf{x}_* , we substitute the approximate posteriors into the predictive distribution $p(\mathbf{f}_*|\mathbf{y}) = \int p(\mathbf{f}_*|\mathbf{u})q(\mathbf{u})d\mathbf{u} = \prod_{c=1}^C \mathcal{N}(f_*^c|\mu_{f_*}^c, \nu_{f_*}^c)$. Thereafter, the distribution of the test label is computed as

$$\begin{aligned} p(y_*|\mathbf{y}) &= \int p(y_*|\mathbf{f}_*)p(\mathbf{f}_*|\mathbf{y})d\mathbf{f}_* \\ &= \int \frac{\exp(f_*^{y_*})}{\sum_{c=1}^C \exp(f_*^c)} \prod_{c=1}^C \mathcal{N}(f_*^c|\mu_{f_*}^c, \nu_{f_*}^c) d\mathbf{f}_*. \end{aligned} \quad (26)$$

The resulting integral however is intractable. Simply, we estimate the mean prediction $p(y_*|y)$ via markov chain monte carlo (MCMC) by drawing samples from the Gaussian $p(\mathbf{f}_*|y)$. Due to the independent latent functions, we draw samples from the posterior $p(\mathbf{f}_*|y)$ as follows: let $\mathbf{t} \sim \mathcal{N}(\mathbf{0}, \mathbf{I})$, we have the sample $\mathbf{x}_\diamond = \boldsymbol{\mu}_{f_*} + \sqrt{\boldsymbol{\nu}_{f_*}} \circ \mathbf{t}$ where the symbol \circ represents the point-wise product.

IV. NUMERICAL EXPERIMENTS

This section verifies the performance of the proposed GPCs (GPC-I, GPC-II, GPC-III and GPCsm) on multiple binary/multi-class classification tasks. We compare them against state-of-the-art scalable GPCs including (i) the binary/multi-class GPC using EP (GPCep) [24], [25] (R codes available at <http://proceedings.mlr.press/v51/herandez-lobato16.html> and <http://proceedings.mlr.press/v70/villacampa-calvo17a.html>), (ii) the binary/multi-class GPC using data augmentation (GPCaug) [30], [31] (Julia codes available at <https://github.com/theogf/AugmentedGaussianProcesses.jl>), and (iii) the binary/multi-class GPC using orthogonally decoupled basis functions (ORTH) [33] (Python codes available at https://github.com/hughsalimbeni/orth_decoupled_var_gps). We run the experiments on a Linux workstation with eight 3.20 GHz cores, nvidia GTX1080Ti, and 32GB memory.

Table I summarizes the capabilities of existing scalable GPCs for handling various likelihoods. Specifically, the GPCep and ORTH employ the probit likelihood for binary case and the step likelihood for multi-class case; and the GPCaug uses the logit likelihood for binary case and the logistic-softmax likelihood¹⁰ for multi-class case.

TABLE I

THE CAPABILITIES OF EXISTING SCALABLE GPCs FOR HANDLING VARIOUS LIKELIHOODS. THE SYMBOL “b” REPRESENTS BINARY CASE AND “m” REPRESENTS MULTI-CLASS CASE. NOTE THAT THE GPCaug EMPLOYS A LOGISTIC-SOFTMAX LIKELIHOOD FOR MULTI-CLASS CASE.

	Step lik.	Probit lik.	Logit lik.	Softmax lik.
GPCep [24], [25]	✓(m)	✓(b)	✗	✗
GPCaug [30], [31]	✗	✗	✓(b)	✓(m)
ORTH [33]	✓(m)	✓(b)	✗	✗
Ours	✓(b, m)	✓(b, m)	✓(b, m)	✓(m)

A. Comparative results

1) *Toy examples*: We showcase the proposed GPCs on two illustrative binary and multi-class cases. The binary case is the `banana` dataset used in [27]; the synthetic three-class case samples three latent functions from a GP prior, and applies the rule $y(\mathbf{x}) = \arg\max_c f^c(\mathbf{x})$ to them. For the two classification datasets, we use $m = 32$ and the Matérn32 kernel for GPCs. The models are trained using the Adam optimizer [37] over 5000 iterations.

As shown in Fig. 2, it is observed that (i) the proposed GPCs well classify the two datasets; and (ii) the variational inference framework pushes the optimized inducing points towards the

¹⁰Similar to the softmax (14), this likelihood expresses as $p(y_i|\mathbf{f}_i) = \sigma(f_i^{y_i}) / \sum_{c=1}^C \sigma(f_i^c)$ with $\sigma(z) = (1 + \exp(-z))^{-1}$.

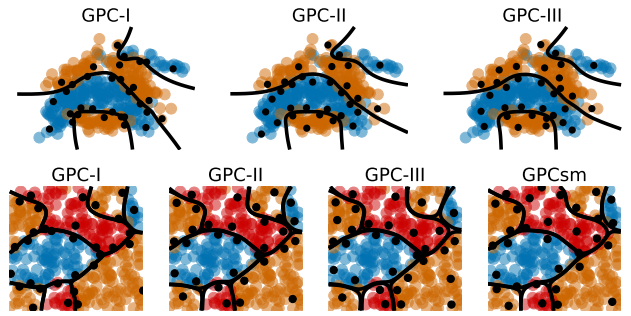


Fig. 2. Illustration of the proposed GPCs on a binary case (top row) and a three-class case (bottom row). The black curves represent the contours at which the predicted class probability is 0.5. The black circles represent the optimized locations of inducing points.

decision boundaries, which is similar to [27] but different from [24], [25].¹¹

2) *UCI benchmarks*: Similar to [33], we conduct the comparison on 19 UCI datasets with $n \in [4897, 130064]$, $d \in [7, 51]$, and $C \in [2, 26]$. The model configurations for comparison are detailed in Appendix D. Table II summarizes the average classification accuracy (acc) and negative log likelihood (nll) results of scalable GPCs on the UCI benchmarks. The complete results on each dataset are provided in Tables III and IV in Appendix E. Note that for the fully-connected neural networks using Selu activations, we use the results reported in [39]. For ORTH, we use the results reported in [33].¹²

It is observed that for binary benchmarks, the proposed three GPCs using different likelihoods outperform the others, and they are competitive in terms of average acc. Besides, compared to the GPC-I using step likelihood, GPC-II and GPC-III have a slightly better performance in terms of nll. As for multi-class benchmarks, all the proposed GPCs outperform the competitors, and particularly, the GPCsm using softmax likelihood provides remarkable performance in terms of nll.

As for GPCep [24], [25], in order to have scalable and analytical ELBO, it employs (i) the FITC assumption $p(\mathbf{f}|\mathbf{u}) = \prod_{i=1}^n p(f_i|\mathbf{u})$, and (ii) an approximation to the integral in (6) of [25]. It is found that EP has a better approximation than VI for standard GPC [13]. The GPCep in our experiments indeed is very competitive, *especially in terms of nll and convergence* (see for example Fig. 4(b)-(d)), in comparison to the proposed GPCs for almost all the datasets except `mushroom`, `nursery` and `wine-quality-white`. The capability of GPCep may be limited, because (i) the additional assumption and approximation may worsen the prediction [23]; and (ii) the R package sometimes is unstable, e.g., it fails in 4 out of the 10 runs on the `mushroom` dataset.

The ORTH has acceptable acc results but provides relatively poor nll results in comparison to GPCep. Finally, the GPCaug exhibits competitive performance on the binary benchmarks. But the multi-class results of GPCaug are not attractive. For

¹¹The FITC assumption in [24], [25] incurs overlapped inducing points. This has also been observed in regression tasks [23].

¹²[33] employs the Matérn52+RBF kernel for ORTH. To be fair, the proposed GPCs use the same combination kernel and produce the results in Table V in Appendix E. It is found that the proposed scalable GPCs outperform ORTH.

TABLE II

AVERAGE CLASSIFICATION ACCURACY (ACC) AND NEGATIVE LOG LIKELIHOOD (NLL) RESULTS ON UCI BENCHMARKS. THE VALUE OF GPCep IN THE BRACKETS INDICATES THE AVERAGE RESULTS FOR ALL THE MULTI-CLASS DATASETS EXCEPT NURSERY. THE VALUE OF GPCaug IN THE BRACKETS INDICATES THE AVERAGE RESULTS FOR ALL THE MULTI-CLASS UCI DATASETS EXCEPT WAVEFORM-NOISE.

		Selu	ORTH	GPCep	GPCaug	GPC-I	GPC-II	GPC-III	GPCsm
binary	acc	92.6	93.0	94.0	94.5	95.1	95.1	95.1	NA
	nll	NA	0.1639	0.1506	0.1354	0.1355	0.1349	0.1349	NA
multi-class	acc	91.1	89.2	87.1 (90.4)	83.0 (87.5)	93.0	93.0	93.0	92.6
	nll	NA	0.5976	1.5637 (0.3168)	0.3844 (0.3196)	0.2374	0.2331	0.2353	0.1858

example, it fails on the `waveform-noise` dataset. Besides, the GPCaug sometimes suffers from slow convergence, see for example Fig. 4(c) and (d). This may be caused by the coordinate ascent optimizer deployed in the GPCaug package.

Finally, the proposed GPCs are much more efficient than GPCaug and GPCep due to the flexible tensorflow framework with GPU acceleration. For instance, the proposed GPCs require around 5 minutes to run on the `miniboone` dataset; while GPCep requires 7.9 hours and GPCaug requires 2.3 hours.

3) *The airline dataset*: We finally assess the performance of the GPCs on the large-scale `airline` dataset containing the information of USA flights between January and April of 2008 [27]. The dataset has eight inputs including age of the aircraft, distance covered, airtime, departure time, arrival time, day of the week, day of the month and month. According to [25], we treat the dataset as a classification task to predict the flight delay with three statuses: on time, more than 5 minutes of delay, or more than 5 minutes before time. We partition the dataset into 2M training points and 10000 test points. We employ the RBF kernel, and use $m = 200$ for the proposed GPCs, GPCep and GPCaug, and $\beta = 200$ and $\gamma = 500$ for ORTH; we run the Adam optimizer over 100000 iterations using a mini-batch size of 1024 and the learning rate of 0.01.

As shown in Fig. 3, the proposed GPCs, especially GPCsm, converge with superior results in terms of both acc and nll. The ORTH provides reasonable acc results, but suffers from poor nll results. In contrast, the GPCep converges with the second best nll results. Finally, the GPCaug has a stable but relatively poor performance on this dataset.

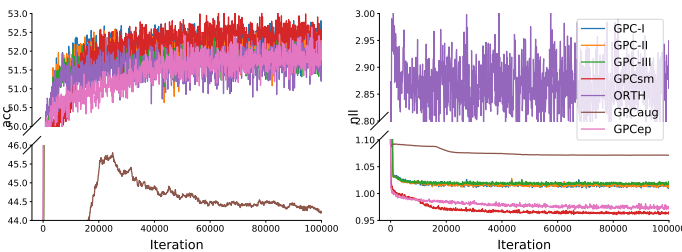


Fig. 3. Comparative results of scalable GPCs on the large-scale `airline` dataset.

B. Discussions of proposed GPCs

1) *Can we use a fixed δ ?*: The parameter δ is originally introduced in the robust step likelihoods (5) and (15). It prevents the logarithm in ELBOs (8) and (18) from being

infinite; and plays the role of noise, like GPR, to be robust to outliers [40]. A fixed δ , e.g., 10^{-3} is suggested by [28], [36] for classification. But we would like to argue that *a fixed δ will worsen the predictive distribution, especially the predictive variance*.

To verify this, we run the proposed GPCs on the binary dataset `adult` and the multi-class dataset `waveform-noise` using a fixed δ and a free δ , respectively, in Fig. 4(a)-(d). Particularly, Fig. 4(e) and (f) showcase the estimations of latent predictive mean $\{\mu_{f_i}\}_{i=1}^n$ and variance $\{\nu_{f_i}\}_{i=1}^n$ in GPC-I using fixed or optimized δ on the `adult` dataset.

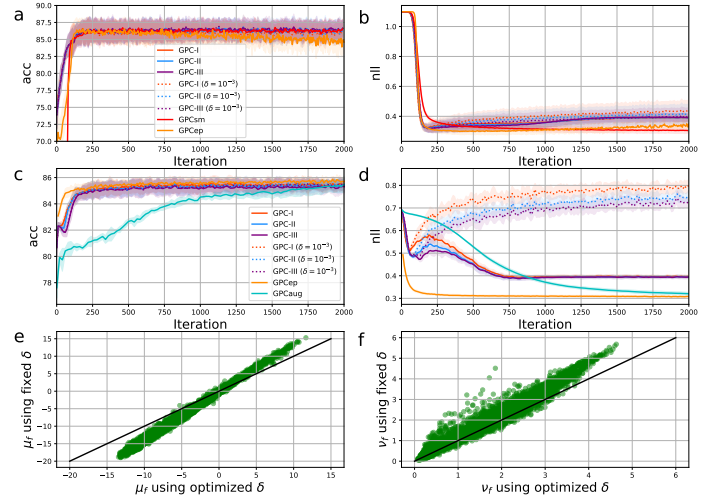


Fig. 4. The accuracy (acc) and negative log likelihood (nll) of scalable GPCs on the multi-class `waveform-noise` dataset (top) and the binary `adult` dataset (medium); the bottom is the $\{\mu_{f_i}\}_{i=1}^n$ and $\{\nu_{f_i}\}_{i=1}^n$ estimated by GPC-I with fixed or optimized δ on the `adult` dataset. Note that the poor results of GPCaug for `waveform-noise` are not included.

We observe that the fixed δ brings a poor nll performance, e.g., it even increases during the training on the `adult` dataset. This phenomenon has also been observed in [25]. Taking the binary GPCs for example, we find that they have an optimum

$$\delta_* = 1 - \frac{1}{n} \sum_{i=1}^n \Phi_{\mathcal{N}} \left(\frac{y_i \mu_{f_i}}{\sqrt{a + \nu_{f_i}}} \right) \quad (27)$$

for the bound (8). When using a fixed δ , the model has to *over-/under-estimate* μ_{f_i} and ν_{f_i} in order to maximize \mathcal{L} , see Fig. 4(e) and (f). These ineffective estimations, especially the overestimated ν_{f_i} , bring poor nll results. Hence, we treat $\delta > 0$ as a free hyperparameter and infer it from data in order to (i)

relieve this issue, see Fig. 4(b) and (d); and (ii) keep the sum formulation in (8), which is crucial for stochastic optimization.

2) *Pros & cons of proposed GPCs*: From the foregoing classification results, we have the following findings:

- It is found that the bounds (8) and (18) for the proposed GPCs using these three likelihoods (step, probit and logit) are expressed uniformly. Hence, the symmetric and bell-shaped error distributions help GPC-I, GPC-II and GPC-III perform similarly. Besides, increasing the noise variance a in Gaussian error (step→probit→logit) brings softer likelihood and slightly better nll results;
- The introduction of δ helps derive analytical ELBOs for GPC-I, GPC-II and GPC-III. And compared to the usage of a fixed δ , optimizing δ significantly improves the nll results. However, it is found that the GPCs using δ have worse nll results than the counterparts on some binary/multi-class datasets, see for example Fig. 4;
- Different from GPC-I, GPC-II and GPC-III, the asymmetric and varying Gumbel errors $\{\epsilon_i\}_{i=1}^n$ help GPCsm describe the *heteroscedasticity*, thus outperforming the others in terms of nll. But the GPCsm may suffer from slow convergence in the early stage due to the complicated model structure, see for example Fig. 4(b).

V. CONCLUSION

This work presents a novel unifying framework which derives analytical ELBO for scalable GPCs using various likelihoods. This is achieved by introducing additive noises to interpret the GPCs in an augmented probability space through the internal variables \mathbf{g} or directly the noises themselves. The superiority of our GPCs has been empirically demonstrated on extensive binary/multi-class classification tasks against state-of-the-art scalable GPCs.

ACKNOWLEDGMENTS

This work was conducted within the Rolls-Royce@NTU Corporate Lab with support from the National Research Foundation (NRF) Singapore under the Corp Lab@University Scheme. It is also partially supported by the Data Science and Artificial Intelligence Research Center (DSAIR) and the School of Computer Science and Engineering at Nanyang Technological University.

APPENDIX A

THE GAUSSIAN APPROXIMATION TO VARIOUS ERROR DISTRIBUTIONS

As discussed before, the step and (multinomial) probit/logit likelihoods can be recovered by varying over different error distributions in the GPC models (3) and (11). Particularly, for the symmetric Dirac-delta, normal and logistic errors, since they are similar, we can describe them using a unifying Gaussian error $\mathcal{N}(\epsilon|0, a)$, resulting in a unifying GPC framework. As illustrated in Fig. 5, the Dirac-delta error can be approximated by letting $a \rightarrow 0$; the logistic error can be approximated by having $a = 2.897$, which is derived by minimizing their maximal CDF difference.

For the skewed Gumbel error, which relates to the specific softmax likelihood for multi-class GPC, we should however tackle it using another strategy, which is detailed in section III-D.

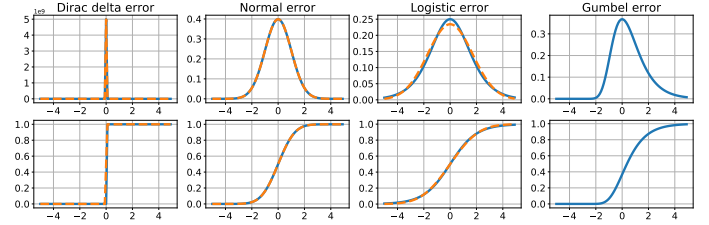


Fig. 5. The error distributions related to various GPC likelihoods. The top row shows the PDF of error distributions, whereas the bottom row shows the CDF. The dash curves represent the Gaussian approximation to the error distributions.

APPENDIX B

TREATING THE NOISE VARIANCE a AS A HYPERPARAMETER?

For the binary GPC with additive noise in section II-B, by treating the noise variance $a \geq 0$ as hyperparameters, we obtain the derivative of \mathcal{L} in (8) w.r.t a as

$$\frac{\partial \mathcal{L}}{\partial a} = -\frac{1}{2} \log \left(\frac{1-\delta}{\delta} \right) \sum_{i=1}^n \left[\phi_{\mathcal{N}} \left(\frac{y_i \mu_{f_i}}{\sqrt{a + \nu_{f_i}}} \right) \frac{y_i \mu_{f_i}}{(a + \nu_{f_i})^{\frac{3}{2}}} \right].$$

It is found that μ_{f_i} represents the prediction mean at \mathbf{x}_i . When the binary GPC provides sensible predictions, we have $y_i \mu_{f_i} > 0$. Hence, we have $\partial \mathcal{L} / \partial a < 0$, which means that the ELBO \mathcal{L} arrives at the maximum when $a = 0$.

Similarly, for the multi-class GPC with additive noise in section III-B, we obtain the derivative of \mathcal{L} in (18) w.r.t a as

$$\frac{\partial \mathcal{L}}{\partial a} = \log \left(\frac{1-\delta}{\delta} (C-1) \right) \sum_{i=1}^n \frac{\partial S_i}{\partial a},$$

where

$$\begin{aligned} \frac{\partial S_i}{\partial a} = & -\frac{1}{2} \mathbb{E}_{g_i^{y_i}} \left[\sum_{c \neq y_i} \frac{g_i^{y_i} - \mu_{f_i}^c}{(a + \nu_{f_i}^c)^{\frac{3}{2}}} \phi_{\mathcal{N}} \left(\frac{g_i^{y_i} - \mu_{f_i}^c}{\sqrt{a + \nu_{f_i}^c}} \right) \right. \\ & \left. \prod_{c' \neq y_i, c} \Phi_{\mathcal{N}} \left(\frac{g_i^{y_i} - \mu_{f_i}^{c'}}{\sqrt{a + \nu_{f_i}^{c'}}} \right) \right] \\ & + \int \frac{\partial \phi_{\mathcal{N}} \left(\frac{g_i^{y_i} - \mu_{f_i}^{y_i}}{\sqrt{a + \nu_{f_i}^{y_i}}} \right)}{\partial a} \prod_{c' \neq y_i} \Phi_{\mathcal{N}} \left(\frac{g_i^{y_i} - \mu_{f_i}^{c'}}{\sqrt{a + \nu_{f_i}^{c'}}} \right) dg_i^{y_i}. \end{aligned}$$

For the first term in the right-hand side of $\partial S_i / \partial a$, since $\Phi_{\mathcal{N}}(x) > \Phi_{\mathcal{N}}(-x)$ and $\phi_{\mathcal{N}}(x) = \phi_{\mathcal{N}}(-x)$ for $x > 0$, we

know that this is a negative term. For the second term in the right-hand side of $\partial S_i/\partial a$, it satisfies

$$\begin{aligned} &< \int \frac{\partial \phi_{\mathcal{N}}\left(\frac{g_i^{y_i} - \mu_{f_i}^{y_i}}{\sqrt{a + \nu_{f_i}^{y_i}}}\right)}{\partial a} dg_i^{y_i} \\ &= -\frac{1}{2} \mathbb{E}_{g_i^{y_i}} \left[\frac{1}{a + \nu_{f_i}^{y_i}} - \frac{(g_i^{y_i} - \mu_{f_i}^{y_i})^2}{(a + \nu_{f_i}^{y_i})^2} \right] = 0. \end{aligned}$$

Hence, we again have $\partial S_i/\partial a < 0$ and furthermore $\partial \mathcal{L}/\partial a < 0$, which means that the ELBO \mathcal{L} arrives at the maximum when $a = 0$.

The above analysis reveals that a cannot play a role of hyperparameter.

APPENDIX C THE ELBO FOR MULTI-CLASS GPC USING SOFTMAX LIKELIHOOD

The original ELBO of multi-class GPC using softmax likelihood in section III-D is

$$\begin{aligned} \mathcal{L} &= \sum_i^n \langle \log p(y_i | \mathbf{f}_i, \epsilon_i) \rangle_{q(\epsilon_i | \mathbf{f}_i) q(\mathbf{f}_i)} - \sum_{i=1}^n \text{KL}(q(\epsilon_i | \mathbf{f}_i) || p(\epsilon_i)) \\ &\quad - \sum_{c=1}^C \text{KL}(q(\mathbf{u}^c | \mathbf{y}) || p(\mathbf{u}^c)). \end{aligned}$$

For the first double-expectation term in the right-hand side of \mathcal{L} , we first calculate the inner expectation as

$$\begin{aligned} &\langle \log p(y_i | \mathbf{f}_i, \epsilon_i) \rangle_{q(\epsilon_i | \mathbf{f}_i)} \\ &= \sum_{c \neq y_i} \int_{-\infty}^{+\infty} q(\epsilon_i | \mathbf{f}_i) \log \Phi_{\mathcal{G}}(\epsilon_i + f_i^{y_i} - f_i^c) d\epsilon_i \\ &= - \sum_{c \neq y_i} \int_{-\infty}^{+\infty} e^{-(\epsilon_i - \log \theta_i) - e^{-(\epsilon_i - \log \theta_i)}} e^{-(\epsilon_i + f_i^{y_i} - f_i^c)} d\epsilon_i \\ &\stackrel{u = \epsilon_i - \log \theta_i}{=} - \sum_{c \neq y_i} \theta_i e^{f_i^c - f_i^{y_i}} \int_0^{+\infty} u e^{-\theta u} du \\ &= \sum_{c \neq y_i} \theta_i e^{f_i^c - f_i^{y_i}} \frac{(1 + \theta u) e^{-\theta u}}{\theta^2} \Big|_0^{+\infty} \\ &= - \frac{1}{\theta_i} \sum_{c \neq y_i} e^{f_i^c - f_i^{y_i}}. \end{aligned}$$

Then, the outside expectation is analytically expressed as

$$\begin{aligned} &\langle \log p(y_i | \mathbf{f}_i, \epsilon_i) \rangle_{q(\epsilon_i | \mathbf{f}_i) q(\mathbf{f}_i)} \\ &= - \frac{1}{\theta_i} \int e^{-f_i^{y_i}} q(f_i^{y_i}) df_i^{y_i} \sum_{c \neq y_i} \int e^{f_i^c} q(f_i^c) df_i^c \\ &= - \frac{1}{\theta_i} \exp\left(\frac{\nu_{f_i}^c}{2} - \mu_{f_i}^c\right) \sum_{c \neq y_i} \exp\left(\frac{\nu_{f_i}^c}{2} + \mu_{f_i}^c\right). \end{aligned}$$

For the KL divergence $\sum_{i=1}^n \text{KL}(q(\epsilon_i | \mathbf{f}_i) || p(\epsilon_i))$ in the right-hand side of \mathcal{L} , we have

$$\sum_{i=1}^n \text{KL}(q(\epsilon_i | \mathbf{f}_i) || p(\epsilon_i)) = \sum_{i=1}^n \left(\log \theta_i + \frac{1}{\theta_i} - 1 \right).$$

For the KL divergence $\sum_{c=1}^C \text{KL}(q(\mathbf{u}^c | \mathbf{y}) || p(\mathbf{u}^c))$ we have

$$\begin{aligned} &:= \frac{1}{2} \sum_{c=1}^C \left(\log \frac{|\mathbf{K}_{mm}^c|}{|\mathbf{S}^c|} - m + \text{tr}[(\mathbf{K}_{mm}^c)^{-1} \mathbf{S}^c] \right. \\ &\quad \left. + (\mathbf{m}^c)^\top (\mathbf{K}_{mm}^c)^{-1} \mathbf{m}^c \right). \end{aligned}$$

According to the above computations, the ELBO is reorganized as

$$\mathcal{L} = \sum_{i=1}^n \left\{ -\frac{1}{\theta_i} \mathcal{P}_i - \log \theta_i - \frac{1}{\theta_i} + 1 \right\} - \sum_{c=1}^C \text{KL}(q(\mathbf{u}^c | \mathbf{y}) || p(\mathbf{u}^c)),$$

with $\mathcal{P}_i = \exp\left(\frac{\nu_{f_i}^{y_i}}{2} - \mu_{f_i}^{y_i}\right) \sum_{c \neq y_i} \exp\left(\frac{\nu_{f_i}^c}{2} + \mu_{f_i}^c\right)$. The double-sum in the right-hand side of \mathcal{L} over data points and classes implies that we could obtain an unbiased estimation of \mathcal{L} via a subset of both data points and classes, which is potential for large categorical cases [41].

APPENDIX D DETAILS FOR UCI EXPERIMENTS

For the experiments on 19 UCI classification benchmarks, similar to [33], we employ the experimental settings detailed as follows.

As for data preprocessing, we use the package *Bayesian Benchmarks*¹³ which normalizes the inputs of datasets to have zero mean and unit variance along each dimension, and randomly chooses 10% of the data as the test set.

As for the kernel function, the results of ORTH in [33] employ a combination of the Matérn52 kernel with length-scale of $0.1\sqrt{d}$ and variance of 5.0, and the RBF kernel with length-scale of \sqrt{d} and variance of 5.0. But for GPCep and GPCaug, since their packages either only support the RBF kernel or have no kernel combination module, we adopt the RBF kernel with length-scale of $0.1\sqrt{d}$ and variance of 5.0 in the comparison. The proposed GPCs also use the RBF kernel in Tables III and IV in Appendix E. Additionally, to compare with ORTH, Table V in Appendix E offers the results of proposed GPCs using the Matérn52+RBF kernel.

As for optimization, we use $m = 300$ inducing points initialized through the k -means technique, and a mini-batch size of 1024. We employ the Adam optimizer for all the scalable GPCs except GPCaug,¹⁴ and run it over 10000 iterations with a learning rate of 0.01. We here do not employ the natural gradient descent (NGD) strategy for optimizing the variational parameters. Because in comparison to the regression task, the NGD+Adam optimizer brings little benefits for classification [33], [38].

Finally, as for likelihoods, the ORTH and GPCep employ the probit likelihood for binary case and the step likelihood for multi-class case; the GPCaug adopts the logit likelihood for binary case and the logistic-softmax likelihood for multi-class case; and our GPCs have no limit and run with all likelihoods.

¹³https://github.com/hughsalimbeni/bayesian_benchmarks.

¹⁴The Julia package of GPCaug employs a coordinate ascent optimizer.

APPENDIX E
DETAILED RESULTS

Tables III and IV provide the average results (over 10 runs) of scalable binary/multi-class GPCs on 19 UCI benchmarks in terms of accuracy and negative log likelihood. Additionally, Table V shows the average results of proposed GPCs using the Matérn52+RBF kernel on 19 UCI benchmarks.

REFERENCES

- [1] C. E. Rasmussen and C. K. Williams, *Gaussian processes for machine learning*. MIT Press, 2006.
- [2] B. Settles, “Active learning literature survey,” *Machine Learning*, vol. 15, no. 2, pp. 201–221, 1994.
- [3] N. Lawrence, “Probabilistic non-linear principal component analysis with Gaussian process latent variable models,” *Journal of Machine Learning Research*, vol. 6, no. Nov, pp. 1783–1816, 2005.
- [4] M. A. Alvarez, L. Rosasco, N. D. Lawrence *et al.*, “Kernels for vector-valued functions: A review,” *Foundations and Trends® in Machine Learning*, vol. 4, no. 3, pp. 195–266, 2012.
- [5] H. Liu, J. Cai, and Y.-S. Ong, “Remarks on multi-output Gaussian process regression,” *Knowledge-Based Systems*, vol. 144, no. March, pp. 102–121, 2018.
- [6] H.-C. Kim and Z. Ghahramani, “Bayesian Gaussian process classification with the EM-EP algorithm,” *IEEE Transactions on Pattern Analysis and Machine Intelligence*, vol. 28, no. 12, pp. 1948–1959, 2006.
- [7] L. Wang and C. Li, “Spectrum-based kernel length estimation for Gaussian process classification,” *IEEE Transactions on Cybernetics*, vol. 44, no. 6, pp. 805–816, 2013.
- [8] J. Quiñero-Candela and C. E. Rasmussen, “A unifying view of sparse approximate Gaussian process regression,” *Journal of Machine Learning Research*, vol. 6, no. Dec, pp. 1939–1959, 2005.
- [9] M. K. Titsias, “Variational learning of inducing variables in sparse Gaussian processes,” in *Artificial Intelligence and Statistics*, 2009, pp. 567–574.
- [10] J. Hensman, N. Fusi, and N. D. Lawrence, “Gaussian processes for big data,” in *Uncertainty in Artificial Intelligence*. Citeseer, 2013, pp. 282–290.
- [11] B. Fröhlich, E. Rodner, M. Kemmler, and J. Denzler, “Large-scale Gaussian process multi-class classification for semantic segmentation and facade recognition,” *Machine Vision and Applications*, vol. 24, no. 5, pp. 1043–1053, 2013.
- [12] D. Milios, R. Camoriano, P. Michiardi, L. Rosasco, and M. Filippone, “Dirichlet-based Gaussian processes for large-scale calibrated classification,” in *Advances in Neural Information Processing Systems*, 2018, pp. 6008–6018.
- [13] H. Nickisch and C. E. Rasmussen, “Approximations for binary Gaussian process classification,” *Journal of Machine Learning Research*, vol. 9, no. Oct, pp. 2035–2078, 2008.
- [14] H. Liu, Y.-S. Ong, X. Shen, and J. Cai, “When Gaussian process meets big data: A review of scalable gps,” *arXiv preprint arXiv:1807.01065*, 2018.
- [15] E. Snelson and Z. Ghahramani, “Sparse Gaussian processes using pseudo-inputs,” in *Advances in Neural Information Processing Systems*, 2006, pp. 1257–1264.
- [16] A. Wilson and H. Nickisch, “Kernel interpolation for scalable structured Gaussian processes (KISS-GP),” in *International Conference on Machine Learning*, 2015, pp. 1775–1784.
- [17] T. N. Hoang, Q. M. Hoang, and B. K. H. Low, “A unifying framework of anytime sparse Gaussian process regression models with stochastic variational inference for big data,” in *International Conference on Machine Learning*, 2015, pp. 569–578.
- [18] H. Peng, S. Zhe, X. Zhang, and Y. Qi, “Asynchronous distributed variational Gaussian process for regression,” in *International Conference on Machine Learning*, 2017, pp. 2788–2797.
- [19] M. D. Hoffman, D. M. Blei, C. Wang, and J. Paisley, “Stochastic variational inference,” *Journal of Machine Learning Research*, vol. 14, no. 1, pp. 1303–1347, 2013.
- [20] G. Pleiss, J. Gardner, K. Weinberger, and A. G. Wilson, “Constant-time predictive distributions for Gaussian processes,” in *International Conference on Machine Learning*, 2018, pp. 4111–4120.
- [21] J. Gardner, G. Pleiss, R. Wu, K. Weinberger, and A. Wilson, “Product kernel interpolation for scalable Gaussian processes,” in *Artificial Intelligence and Statistics*, 2018, pp. 1407–1416.
- [22] A. Naish-Guzman and S. Holden, “The generalized FITC approximation,” in *Advances in Neural Information Processing Systems*, 2008, pp. 1057–1064.
- [23] M. Bauer, M. van der Wilk, and C. E. Rasmussen, “Understanding probabilistic sparse Gaussian process approximations,” in *Advances in Neural Information Processing Systems*, 2016, pp. 1533–1541.
- [24] D. Hernández-Lobato and J. M. Hernández-Lobato, “Scalable Gaussian process classification via expectation propagation,” in *Artificial Intelligence and Statistics*, 2016, pp. 168–176.
- [25] C. Villacampa-Calvo and D. Hernández-Lobato, “Scalable multi-class Gaussian process classification using expectation propagation,” in *International Conference on Machine Learning*. JMLR. org, 2017, pp. 3550–3559.
- [26] Y. Li, J. M. Hernández-Lobato, and R. E. Turner, “Stochastic expectation propagation,” in *Advances in Neural Information Processing Systems*, 2015, pp. 2323–2331.
- [27] J. Hensman, A. Matthews, and Z. Ghahramani, “Scalable variational gaussian process classification,” in *Artificial Intelligence and Statistics*, 2015, pp. 351–360.
- [28] J. Hensman, A. G. Matthews, M. Filippone, and Z. Ghahramani, “MCMC for variationally sparse Gaussian processes,” in *Advances in Neural Information Processing Systems*, 2015, pp. 1648–1656.
- [29] N. G. Polson, J. G. Scott, and J. Windle, “Bayesian inference for logistic models using pólya–Gamma latent variables,” *Journal of the American Statistical Association*, vol. 108, no. 504, pp. 1339–1349, 2013.
- [30] F. Wenzel, T. Galy-Fajou, C. Donner, M. Kloft, and M. Opper, “Efficient Gaussian process classification using pólya-gamma data augmentation,” in *International Conference on Machine Learning*, 2018.
- [31] T. Galy-Fajou, F. Wenzel, C. Donner, and M. Opper, “Multi-class gaussian process classification made conjugate: Efficient inference via data augmentation,” in *International Conference on Artificial Intelligence and Statistics*, 2019.
- [32] C.-A. Cheng and B. Boots, “Variational inference for Gaussian process models with linear complexity,” in *Advances in Neural Information Processing Systems*, 2017, pp. 5184–5194.
- [33] H. Salimbeni, C.-A. Cheng, B. Boots, and M. Deisenroth, “Orthogonally decoupled variational Gaussian processes,” in *Advances in Neural Information Processing Systems*, 2018, pp. 8711–8720.
- [34] D. G. Matthews, G. Alexander, M. Van Der Wilk, T. Nickson, K. Fujii, A. Boukouvalas, P. León-Villagrà, Z. Ghahramani, and J. Hensman, “GPflow: A Gaussian process library using tensorflow,” *Journal of Machine Learning Research*, vol. 18, no. 1, pp. 1299–1304, 2017.
- [35] S. R. Bowling, M. T. Khasawneh, S. Kaewkuekool, and B. R. Cho, “A logistic approximation to the cumulative normal distribution,” *Journal of Industrial Engineering and Management*, vol. 2, no. 1, 2009.
- [36] A. G. de Garis Matthews, “Scalable Gaussian process inference using variational methods,” *Department of Engineering, University of Cambridge*, 2016.
- [37] D. P. Kingma and J. Ba, “Adam: A method for stochastic optimization,” *arXiv preprint arXiv:1412.6980*, 2014.
- [38] H. Salimbeni, S. Eleftheriadis, and J. Hensman, “Natural gradients in practice: Non-conjugate variational inference in Gaussian process models,” in *International Conference on Artificial Intelligence and Statistics*, 2018, pp. 689–697.
- [39] G. Klambauer, T. Unterthiner, A. Mayr, and S. Hochreiter, “Self-normalizing neural networks,” in *Advances in Neural Information Processing Systems*, 2017, pp. 971–980.
- [40] H.-C. Kim and Z. Ghahramani, “Outlier robust Gaussian process classification,” in *Joint IAPR International Workshops on Statistical Techniques in Pattern Recognition (SPR) and Structural and Syntactic Pattern Recognition (SSPR)*. Springer, 2008, pp. 896–905.
- [41] F. J. Ruiz, M. K. Titsias, A. B. Dieng, and D. M. Blei, “Augment and reduce: Stochastic inference for large categorical distributions,” in *International Conference on Machine Learning*, 2018, pp. 4400–4409.

TABLE III

AVERAGE CLASSIFICATION ACCURACY (ACC) RESULTS ON 19 UCI BENCHMARKS. NOTE THAT ALL THE GPCs EXCEPT ORTH USE THE RBF KERNEL IN THIS COMPARISON. THE RESULTS OF ORTH REPORTED IN [33] EMPLOY THE MATÉRN52+RBF KERNEL.

	n	d	C	Selu	ORTH	GPCep	GPCaug	GPC-I	GPC-II	GPC-III	GPCsm
adult	48842	15	2	84.67	85.65	85.64	85.60	85.53	85.47	85.55	NA
connect-4	67557	43	2	88.07	85.99	84.40	81.28	84.86	84.68	84.52	NA
magic	19020	11	2	86.92	89.35	99.89	99.64	99.89	99.92	99.90	NA
miniboone	130064	51	2	93.07	93.49	99.77	99.87	99.89	99.92	99.92	NA
mushroom	8124	22	2	100.00	100.00	92.03	100.00	99.98	99.98	99.98	NA
ringnorm	7400	21	2	97.51	98.78	98.43	97.62	98.22	98.35	98.34	NA
twonorm	7400	21	2	98.05	97.65	97.78	97.78	97.45	97.49	97.58	NA
chess-krvk	28056	7	18	88.05	67.76	99.89	88.39	99.82	99.78	99.72	99.85
letter	20000	17	26	97.26	95.77	95.43	83.76	96.50	96.66	96.49	96.25
nursery	12960	9	5	99.78	97.30	50.64	92.67	99.99	99.98	99.99	99.63
page-blocks	5473	11	5	95.83	97.21	97.41	96.02	97.06	97.26	97.03	97.10
pendigits	10992	17	10	97.06	99.66	99.36	98.53	99.50	99.58	99.59	99.45
statlog-landsat	6435	37	6	91.00	91.28	92.55	85.68	93.37	93.76	93.70	91.91
statlog-shuttle	58000	10	7	99.90	99.90	99.92	99.70	99.93	99.91	99.90	99.88
thyroid	7200	22	3	98.16	99.47	99.33	94.83	99.29	99.39	99.39	99.21
wall-following	5456	25	4	90.98	95.56	96.78	88.42	96.96	96.70	96.72	96.50
waveform	5000	22	3	84.80	86.13	84.96	86.52	86.86	87.02	87.34	87.84
waveform-noise	5000	41	3	86.08	82.93	85.88	33.40	85.16	85.30	85.54	86.24
wine-quality-white	4898	12	7	63.73	57.05	42.90	48.49	61.22	60.65	60.51	57.24

TABLE IV

AVERAGE NEGATIVE LOG LIKELIHOOD (NLL) RESULTS ON 19 UCI BENCHMARKS. NOTE THAT ALL THE GPCs EXCEPT ORTH USE THE RBF KERNEL IN THIS COMPARISON. THE RESULTS OF ORTH REPORTED IN [33] EMPLOY THE MATÉRN52+RBF KERNEL.

	n	d	C	ORTH	GPCep	GPCaug	GPC-I	GPC-II	GPC-III	GPCsm
adult	48842	15	2	0.3045	0.3074	0.3306	0.3971	0.3956	0.3933	NA
connect-4	67557	43	2	0.3086	0.3822	0.4534	0.3958	0.3998	0.4029	NA
magic	19020	11	2	0.2658	0.0039	0.0153	0.0041	0.0030	0.0029	NA
miniboone	130064	51	2	0.1618	0.0031	0.0064	0.0046	0.0028	0.0029	NA
mushroom	8124	22	2	0.0009	0.2363	0.0054	0.0004	0.0004	0.0004	NA
ringnorm	7400	21	2	0.0466	0.0507	0.0739	0.0568	0.0593	0.0619	NA
twonorm	7400	21	2	0.0590	0.0707	0.0625	0.0898	0.0831	0.0802	NA
chess-krvk	28056	7	18	2.1625	0.0236	0.1918	0.0141	0.0169	0.0223	0.0072
letter	20000	17	26	0.2276	0.1934	0.6852	0.1685	0.1699	0.1789	0.1528
nursery	12960	9	5	0.2225	15.2799	0.1546	0.0042	0.0074	0.0070	0.0299
page-blocks	5473	11	5	0.1328	0.0763	0.1343	0.1314	0.1165	0.1226	0.0896
pendigits	10992	17	10	0.0209	0.0258	0.1095	0.0225	0.0223	0.0232	0.0282
statlog-landsat	6435	37	6	0.3956	0.2148	0.3356	0.2280	0.2164	0.2195	0.2110
statlog-shuttle	58000	10	7	0.0049	0.0035	0.0179	0.0036	0.0041	0.0047	0.0045
thyroid	7200	22	3	0.0115	0.0205	0.0893	0.0296	0.0285	0.0293	0.0245
wall-following	5456	25	4	0.1514	0.0839	0.3437	0.1124	0.1187	0.1242	0.1033
waveform	5000	22	3	0.5640	0.4641	0.3342	0.4097	0.3987	0.3948	0.2832
waveform-noise	5000	41	3	0.7096	0.3170	1.0980	0.4437	0.4295	0.4223	0.2999
wine-quality-white	4898	12	7	2.5681	2.0612	1.1191	1.2806	1.2684	1.2748	0.9953

TABLE V

AVERAGE RESULTS OF PROPOSED GPCs ON 19 UCI BENCHMARKS USING THE MATÉRN52+RBF KERNEL. NOTE THAT THE PROPOSED GPCs PROVIDE RELATIVELY POOR RESULTS ON THE `CONNECT-4` DATASET, WHICH SKEW THE AVERAGE PERFORMANCE.

	n	d	C	acc				nll			
				GPC-I	GPC-II	GPC-III	GPCsm	GPC-I	GPC-II	GPC-III	GPCsm
adult	48842	15	2	85.75	85.86	85.76	NA	0.3921	0.3892	0.3900	NA
connect-4	67557	43	2	76.43	76.49	76.38	NA	0.5393	0.5383	0.5396	NA
magic	19020	11	2	99.89	99.94	99.95	NA	0.0038	0.0029	0.0024	NA
miniboone	130064	51	2	99.87	99.93	99.92	NA	0.0049	0.0028	0.0030	NA
mushroom	8124	22	2	100.00	100.00	100.00	NA	0.0001	0.0001	0.0002	NA
ringnorm	7400	21	2	98.23	98.32	98.35	NA	0.0568	0.0597	0.0624	NA
twonorm	7400	21	2	97.45	97.49	97.64	NA	0.0932	0.0830	0.0798	NA
chess-krvk	28056	7	18	99.67	99.66	99.64	99.80	0.0277	0.0275	0.0290	0.0076
letter	20000	17	26	95.91	96.28	96.26	96.36	0.2101	0.2008	0.2041	0.1433
nursery	12960	9	5	97.54	97.54	97.54	99.95	0.1500	0.1502	0.1504	0.0120
page-blocks	5473	11	5	97.83	97.79	97.85	97.66	0.0990	0.0934	0.0903	0.0745
pendigits	10992	17	10	99.55	99.60	99.62	99.45	0.0226	0.0211	0.0218	0.0255
statlog-landsat	6435	37	6	93.65	93.90	93.77	92.80	0.2189	0.2043	0.2037	0.1900
statlog-shuttle	58000	10	7	99.94	99.94	99.94	99.93	0.0028	0.0030	0.0033	0.0029
thyroid	7200	22	3	99.25	99.42	99.38	99.46	0.0269	0.0236	0.0231	0.0178
wall-following	5456	25	4	97.82	97.78	97.75	97.66	0.0727	0.0733	0.0763	0.0694
waveform	5000	22	3	86.96	86.84	86.96	88.06	0.4130	0.4058	0.4000	0.2828
waveform-noise	5000	41	3	84.86	85.36	85.66	86.22	0.4551	0.4280	0.4224	0.2995
wine-quality-white	4898	12	7	60.71	60.51	60.96	58.20	1.2662	1.2623	1.2573	0.9868
binary (average)				93.9	94.0	94.0	NA	0.1557	0.1537	0.1539	NA
multi-class (average)				92.8	92.9	92.9	93.0	0.2471	0.2411	0.2401	0.1760